ROYAL SOCIETY OF CHEMISTRY

PAPER

Check for updates

Aqueous solutions of super reduced polyoxotungstates as electron storage systems†

Tingting Zhao, Nicola L. Bell, [iD] Greig Chisholm, [iD] Balamurugan Kandasamy, De-Liang Long [iD] and Leroy Cronin [iD] *

Due to the increasing energy density demands of battery technology, it is vital to develop electrolytes with high electron storage capacity. Polyoxometalate (POM) clusters can act as electron sponges, storing and releasing multiple electrons and have potential as electron storage electrolytes for flow batteries. Despite this rational design of clusters for high storage ability can not yet be achieved as little is known about the features influencing storage ability. Here we report that the large POM clusters, $\{P_5W_{30}\}$ and $\{P_8W_{48}\}$, can store up to 23 e⁻ and 28 e⁻ per cluster in acidic aqueous solution, respectively. Our investigations reveal key structural and speciation factors influencing the improved behaviour of these POMs over those previously reported (P_2W_{18}). We show, using NMR and MS, that for these polyoxotungstates hydrolysis equilibria for the different tungstate salts is key to explaining unexpected storage trends while the performance limit for $\{P_5W_{30}\}$ and $\{P_8W_{48}\}$, can be attributed to unavoidable hydrogen generation, evidenced by GC. NMR spectroscopy, in combination with the MS analysis, provided experimental evidence for a cation/proton exchange process during the reduction/reoxidation process of $\{P_5W_{30}\}$ which likely occurs due to this hydrogen generation. Our study offers a deeper understanding of the factors affecting the electron storage ability of POMs and provides insights allowing for further development of these materials for energy storage.

Broader context

The storage of electrons by liquid electrolytes is the critical component of a flow battery. The material needs to be stable, safe, and to store as much charge as possible without loss. The benefits of flow batteries include the ability to recharge them by removing the liquid electrolyte and the potential for coupling them into chemical processes. Traditional flow battery electrolytes have been either simple salts or organic molecules, but these can only store 1–2 electrons per molecule and either suffer from stability issues or are corrosive. Recently it was postulated that high nuclearity polyoxometalate clusters could be used to store a large number of electrons per molecule in aqueous solution. In this study we show that large POM clusters, $\{P_5W_{30}\}$ and $\{P_8W_{48}\}$, can store more than 20 electrons per cluster and we explore the mechanism of electron uptake as well as characterize the solutions as potential electrolytes suitable for use in flow batteries.

Introduction

The transition to a green economy necessitates the development of novel energy storage solutions and there is currently a great deal of interest in redox flow batteries (RFBs) for this application.[1] Vanadium metal oxides have dominated the field however their commercial development has been limited by their low energy density.[2] Two key features are salient when

optimising RFB performance: (1) potential difference between the materials oxidised and reduced and (2) storage capacity.[3,4] Significant work has been undertaken to address the former using different redox pairs.[5] Maximising capacity, or the number of electrons able to be stored and released by a material is still an important area of development.[6] Polyoxometalates (POMs), are a class of early transition metal oxide clusters with MO_x (x = 5, 6) as basic construction units, which can both store and release multiple electrons due to the reduction and oxidation of high-valence transition metals, like W, Mo and V.[7–10] Polyoxometalates are highly soluble yielding tungsten concentrations of up to 8 M for PW_{12}. Hence, investigating how POMs store and release electrons, and how this relates to their structure, will allow for the further exploitation of their unique properties.

School of Chemistry, University of Glasgow, University Avenue, Glasgow, G12 8QQ, UK. E-mail: lee.cronin@glasgow.ac.uk

† Electronic supplementary information (ESI) available. CCDC 2173983. For ESI and crystallographic data in CIF or other electronic format see DOI: https://doi.org/10.1039/d3ee00569k

This journal is © The Royal Society of Chemistry 2023

Energy Environ. Sci., 2023, **16**, 2603–2610 | 2603

The exceptional electron storage ability of POMs was first hinted at when Launay reported the reduction of $[H_2W_{12}O_{40}]^{6-}$, suggesting the reduction of the cluster by six electrons was also accompanied by the transfer of six protons.[11,12] Bond *et al.* also reported the reduction of the Wells–Dawson $[S_2Mo_{18}O_{62}]^{4-}$ anion in a mixture of acetonitrile and water solution, indicating eight reversible one-electron reductions of this anion.[13] A leap to 24 electron reduction was achieved by Yoshikawa and Awaga, who investigated a Keggin-type POM, $[PMo_{12}O_{40}]^{3-}$ as a cathode active material.[14] Through X-ray absorption near-edge structure technique analysis they found all 12 Mo^{6+} centres in this Keggin structure were reduced to Mo^{4+} in the discharging process, which means this Keggin can store 24 e^- per cluster. But this performance was achieved in the solid state and not aqueous solution. Since many energy storage devices use aqueous solutions as electrolytes, understanding the electron storage ability of POMs in aqueous solution is important.[1,15] Normally in aqueous solution, the electron storage ability is limited by side reactions, like hydrogen evolution, as the reduction of these polyoxoanions occurs at only slightly less cathodic potentials than hydrogen evolution as more electrons are put into system. This means it becomes harder to further reduce the POMs and side reactions become an even larger problem.

In previous work we demonstrated that the POM cluster, $Li_6[P_2W_{18}O_{62}]$, has exceptional proton-coupled electron redox activity and can reversibly accept up to 18 protons and electrons in aqueous solution at high concentration and low pH.[16,17] It is therefore of interest to examine whether this concentration and pH effect applies to other POMs offering the opportunity to increase the storage capacity by utilizing larger clusters. Also, inspired by this initial finding, it is important to investigate if electron storage potential can scale with cluster nuclearity and what properties of a cluster promote electron storage. Therefore, we selected two other phosphotungstates, $[NaP_5W_{30}O_{110}]^{14-}$ (abbreviated $\{P_5W_{30}\}$) and $[H_7P_8W_{48}O_{184}]^{33-}$ (abbreviated $\{P_8W_{48}\}$). $\{P_5W_{30}\}$, known as the Preyssler anion, has approximate D_{5h} symmetry and consists of a cyclic assembly of five $\{PW_6O_{22}\}$ units. $\{P_5W_{30}\}$ is stable within the pH window from 0 to 11 and is reducible to a blue-coloured species, which make it a promising candidate for multi-electron storage.[18–20] $\{P_8W_{48}\}$ is a wheel-shaped polyoxotungstate which is stable in pH range 1 to 8; it is also a potential candidate for multi-electron storage.[21] Previous studies show that the electrochemistry of POMs is dependent on the molecular charge, charge density,[22] cation type, and cation/anion size.[23,24] Therefore, as $\{P_5W_{30}\}$ and $\{P_8W_{48}\}$ have bigger size and higher charge density than $\{P_2W_{18}\}$, the effect of these factors on the electron storage ability suggest that they should be great candidates to test our hypothesis to assess how many electrons can be stored in a single cluster molecule.

To explore the mechanism of reduction to form highly-reduced POMs, previous work suggests it is important to consider the aggregation of polyoxoanions in solution. This can be done by small-angle X-ray scattering (SAXS) *e.g.*, for $[PW_{12}O_{40}]^{3-}$ and $[P_2W_{18}O_{62}]^{6-}$.[14,17] Furthermore, we reasoned that NMR should also be a powerful technique to study the structure in solution as a function of different redox state.[25–27] For example, ^7Li NMR has been used to analyse the mechanism

of Li-ion battery charging and discharging processes.[25,26] More recently, NMR was used to monitor POMs cation–anion interaction in solution. Nyman and co-workers investigated ion-pairing between Cs^+ cations and Nb/Ta POM anions using inversion-recovery ^{133}Cs-NMR spectroscopy demonstrating that strong covalent orbital overlap occurs between the alkali metal and the metal oxide ligands.[28,29] Bloor and Kidd studied the ^{39}K NMR chemical shifts in aqueous solutions with different POM anions and concluded that orbital overlap with metal oxides can decrease paramagnetic shielding of the alkali metal ion relative to solvated ions.[30] However, there is no NMR study to date of the interactions of Li^+ counter cations with polyoxoanions, nor investigations of their behaviour upon reduction of the metal centre.
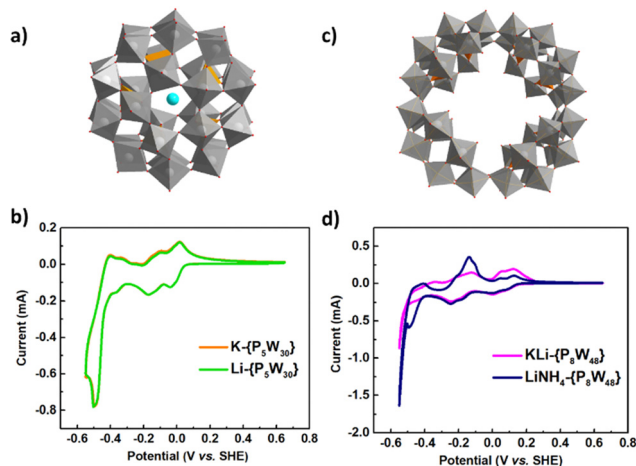
Here, we show that both polyoxoanions $\{P_5W_{30}\}$ and $\{P_8W_{48}\}$ demonstrate notable proton-coupled electron redox processes, which allow the two clusters to reversibly accept up to 23 and 28 e^- per cluster respectively in acidic aqueous solution. The electron storage ability is concentration based and dependent upon the type of counter cations. The excellent electrochemical performance is attributed to both aggregation of reduced polyoxoanions and their protonation in solution, which was studied by ^7Li and ^1H NMR. We also found there is performance limit regarding the total W atoms in the structure, for both $\{P_5W_{30}\}$ and $\{P_8W_{48}\}$, and the possible reasons were analysed including cluster decomposition, competitive hydrogen generation and the effect of different metal coordination environments within the POMs. The ability for these clusters to readily be so highly reduced has importance for the development of new energy storage materials as well as new strategies to develop multi-electron storage systems.

Results and discussion

Synthesis and cyclic voltammetry

K-$\{P_5W_{30}\}$ ($K_{14}[NaP_5W_{30}O_{110}]\cdot22H_2O$) was synthesized according to a modified literature procedure.[19,31] Li-$\{P_5W_{30}\}$ ($Li_{14}[NaP_5W_{30}O_{110}]\cdot38H_2O$) was synthesized by ion exchange of K-$\{P_5W_{30}\}$ in excess $LiNO_3$ and characterized by single crystal XRD structure determination. Refinement of the diffraction data for Li-$\{P_5W_{30}\}$ revealed the structure of polyoxoanion of $[NaP_5W_{30}O_{110}]^{14-}$, with comparable unit cell parameters to those of K-$\{P_5W_{30}\}$ (Fig. 1a and Table S4, ESI†).[18] The redox chemistry of $\{P_5W_{30}\}$ in sulfuric acid solution was studied by cyclic voltammetry (CV) experiments (Fig. 1b). At low concentration (2 mM), K-$\{P_5W_{30}\}$ shows four reversible waves within the -0.6 V to 0.6 V range (*versus* standard hydrogen electrode, SHE). Upon moving to higher concentrations of the POM (10 mM), we found there is significant enhancement in the current intensity of the redox waves for K-$\{P_5W_{30}\}$ when compared with the control study at a concentration of 2 mM (Fig. S15, ESI†) in line with our previous studies.[16] The CV curves for K-$\{P_5W_{30}\}$ and Li-$\{P_5W_{30}\}$ show similar reduction and oxidation waves at 10 mM concentration suggesting that cations may have minimal interaction with the POM in acidic solution.

2604 | *Energy Environ. Sci.*, 2023, **16**, 2603–2610

This journal is © The Royal Society of Chemistry 2023

Fig. 1 (a) Structure of Li-$\{P_5W_{30}\}$ by single crystal XRD (grey polyhedra: W; red ball: O; orange polyhedra: P; cyan ball: Na)[18] (b) cyclic voltammograms of K-$\{P_5W_{30}\}$ (10 mM) and Li-$\{P_5W_{30}\}$ (10 mM) in 1 M H_2SO_4.[18] (c) structure of KLi-$\{P_8W_{48}\}$[21] by single crystal XRD (grey polyhedra: W, red ball: O; orange polyhedra: P), (d) cyclic voltammograms of KLi-$\{P_8W_{48}\}$ (10 mM) and LiNH$_4$-$\{P_8W_{48}\}$ (10 mM) in 1 M H_2SO_4.[32] Scan rate: 10 mV s^{-1}. (See ESI† Section 4.1 for further details)

Similarly, mixed cation salts $K_{28}Li_5H_7[P_8W_{48}O_{184}]\cdot 92H_2O$ (KLi-$\{P_8W_{48}\}$) and $Li_{17}(NH_4)_{21}H_2[P_8W_{48}O_{184}]\cdot 85H_2O$ (LiNH$_4$-$\{P_8W_{48}\}$) were synthesized according to modified literature procedures and the structure of KLi-$\{P_8W_{48}\}$ is shown in Fig. 1c.[21] CV curves of KLi-$\{P_8W_{48}\}$ and LiNH$_4$-$\{P_8W_{48}\}$ (Fig. 1d) show different wave shapes, indicating potential different redox mechanisms, with the LiNH$_4$-$\{P_8W_{48}\}$ salt displaying similar reduction behaviour down to −0.4 V but slightly different oxidation behaviour *cf.* the KLi salt, suggesting different cation incorporation, modulating behaviour, upon reduction including hydrogen evolution which will be further detailed below.[32] However, many of the differences, including the large oxidation peak at ca −0.15 V likely arise from the presence of $[NH_4^+]$ ions.

Flow-cell testing

Previous studies showed the storage of multiple electrons in Li-$\{P_2W_{18}\}$ was proton-coupled, and as the concentration of Li-$\{P_2W_{18}\}$ increased, an increasing number of electrons could be stored. To explore if this trend is followed here we explored the cluster redox performance in a three-electrode electrochemical flow cell with an Hg/HgSO$_4$ as a reference electrode.[16] This device can quantify the number of electrons that the polyoxometalate solutions could store. The oxygen evolution reaction (see Fig. S14, ESI†) was used to be the counterpart reaction of the POM reduction reaction. Water is oxidized and simultaneously produces O_2, protons and electrons ($2H_2O \rightarrow O_2 + 4H^+ + 4e^-$). The protons generated can cross over Nafion membrane and combine with electrons drawn from the external circuit to protonate and reduce an aqueous solution of $[NaP_5W_{30}O_{110}]^{14-}$ on the right-hand side of this cell, forming reduced polyoxoanion $[NaP_5W_{30}O_{110}]^{(14+n)-}$ (n = equivalents of electrons charged). Once the desired number of electrons per cluster had been stored, the reduced POM solution was then re-oxidized

electrochemically in a neighbour cell on the right-hand side sharing the same POM solution. The electrons stored reversibly in the POM solution could be deduced by comparing the total charge (electrons) input to reduce the POM with the charge (electrons) released out when it was re-oxidized.

$\{P_5W_{30}\}$ electron storage capacity studies

The electron storage ability of K-$\{P_5W_{30}\}$ was studied *versus* concentration (Fig. 2a and Fig. S16 and Table S5, ESI†). When increasing the concentration from 2 mM to 5 mM in water (the pH decreased from 4.2 to 3.7 accordingly), the electron storage ability of K-$\{P_5W_{30}\}$ increased from 15.7 e$^-$ to 20.7 e$^-$. The trend at lower concentration is similar to that observed for the previously reported Li-$\{P_2W_{18}\}$,[16] however the trend breaks down above 5 mM as the 10 mM solution (20.7 e$^-$) did not show an increase in performance over the 5 mM one (20.7 e$^-$). Considering the effect of pH,[33] we dissolved the cluster in 0.2 M H_2SO_4 which led to an increase in the solutions storage capacity
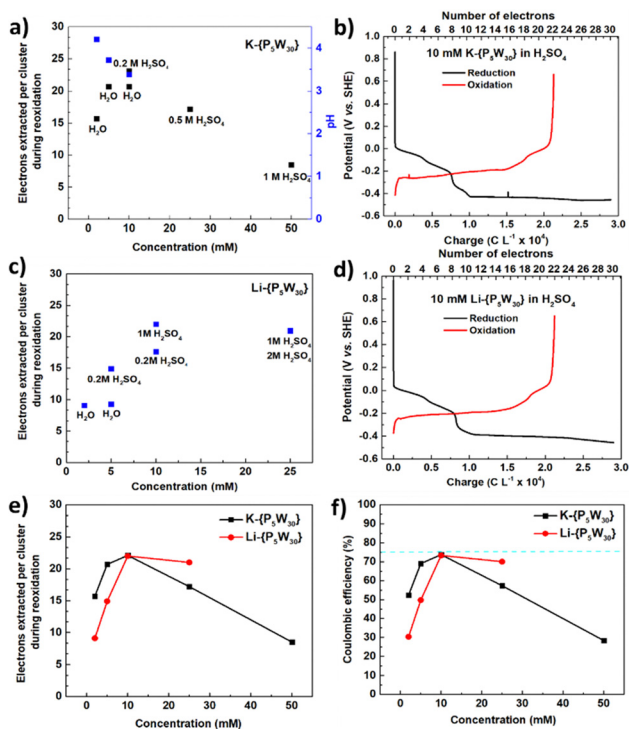
Fig. 2 Reversible multi-electron redox chemistry of $[NaP_5W_{30}O_{110}]^{14-}$. (a) Relationship between K-$\{P_5W_{30}\}$ concentration, solution pH (measured before electro-reduction) and the number of electrons that can be extracted from a reduced solution. Solutions were charged 30 electrons. (b) Representative 23 e$^-$ reduction/reoxidation curves of a 10 mM solution of K-$\{P_5W_{30}\}$, 0.2 M H_2SO_4 was used as supporting electrolyte. (c) Relationship between Li-$\{P_5W_{30}\}$ concentration, and the number of electrons that can be extracted from a reduced solution. (d) Representative 22 e$^-$ reduction/reoxidation curves of a 10 mM solution of Li-$\{P_5W_{30}\}$, 1 M H_2SO_4 was used as supporting electrolyte. In (a) and (c), the number of electrons used to reduce the K-$\{P_5W_{30}\}$ and Li-$\{P_5W_{30}\}$ was 30 per cluster. In (b) and (d), a current density of ±10 mA cm^{-2} was applied. A comparison of K-$\{P_5W_{30}\}$ and Li-$\{P_5W_{30}\}$: (e) electrons extracted *vs.* concentration; (f) coulombic efficiency (the total charge extracted out of the total charge put into the POM solutions) *vs.* concentration.

This journal is © The Royal Society of Chemistry 2023

Energy Environ. Sci., 2023, **16**, 2603–2610 | **2605**

to 22.1 e⁻ (a comparison of 10 mM K-{P₅W₃₀} in H₂O, 0.2 M H₂SO₄ and 0.2 M Li₂SO₄ can be seen in Fig. S18, ESI†), however upon increasing the concentration further to 25 mM and 50 mM the performance decreased to 17.2 and 8.5 e⁻ respectively. A representative 23 e⁻ reduction/reoxidation curves of a 10 mM solution of K-{P₅W₃₀} in 0.2 M H₂SO₄ with the best performance in this group is shown in Fig. 2b.

Lithium salts often have better aqueous solubility than the corresponding potassium salts and some previous studies showed small cations such as Li⁺ can stabilise the reduction of POMs.[23] Therefore we synthesized Li-{P₅W₃₀} with the expectation this system might show better performance than K-{P₅W₃₀}. However, after conducting flow cell tests under low concentration of 2 mM, it was shown to only store 9.1 e⁻ per cluster, while the 5 mM solution can only store 9.3 e⁻ per cluster (Fig. 2c and Fig. S19 and Table S6, ESI†). We were surprised that the performance is even lower than the K salt given our previous work with Li-P₂W₁₈, but upon investigating the ³¹P NMR of this salt in D₂O we found that this cluster degraded readily in solution. In contrast a solution in D₂SO₄ showed no degradation (Fig. S20, ESI†). Thus, H₂SO₄ was used as supporting electrolyte in experiments and the effect of acid was studied. A 5 mM solution of Li-{P₅W₃₀} in 0.2 M H₂SO₄ was able to store 14.9 e⁻, while a 10 mM solution was shown to store 18.0 e⁻. Increasing the acid concentration to 1 M while maintaining Li-{P₅W₃₀} at 10 mM allowed storage of up to 22.0 e⁻. At 25 mM substrate in 1 M acid, we found the performance dropped slightly to 21.0 e⁻ and performance was not increased by further increasing acid concentration to 2 M. Thus, it seems these conditions represent the performance limit of Li-{P₅W₃₀}, and the representative reduction/reoxidation curves are shown in Fig. 2d. In total, the electron storage ability of Li-{P₅W₃₀} is affected by both concentrations of POM and supporting acid, increasing with greater concentration of POM from 2 mM to 10 mM and with decreasing pH. However, increasing the concentration further to 25 mM or lowering pH, does not improve the performance more. A comparison of K-{P₅W₃₀} and Li-{P₅W₃₀} with respect to extracted electrons and coulombic efficiency is shown in Fig. 2e and 2f. Both K-{P₅W₃₀} and Li-{P₅W₃₀} show a similar trend of first increasing and then decreasing with a peak performance under 10 mM. In total, K-{P₅W₃₀} is better than Li-{P₅W₃₀} in terms of electron storage ability and coulombic efficiency under lower concentration however Li-{P₅W₃₀} begins to show an advantage under higher concentration.

{P₈W₄₈} electron storage capacity studies

Next the electron storage ability of the larger tungstate wheel, KLi-{P₈W₄₈}, was studied as a function of concentration (Fig. 3a and Fig. S21 and Table S7, ESI†). Here 1 M H₂SO₄ was used as the supporting electrolyte for all flow cell tests to overcome the lower solubility of KLi-{P₈W₄₈} in H₂O. Since {P₂W₁₈} was effectively charged with 18 e⁻ and {P₅W₃₀} was able to be charged with 30 e⁻ we elected to first charging 48 e⁻ per cluster for this salt (i.e. assuming each W^VI can be reduced to W^V). At this level of charge the POM shows decomposition with a rapid decrease in electrochemical performance (Fig. S21, ESI,† 25 mM charge 48 e⁻ one). After observing the charge curve
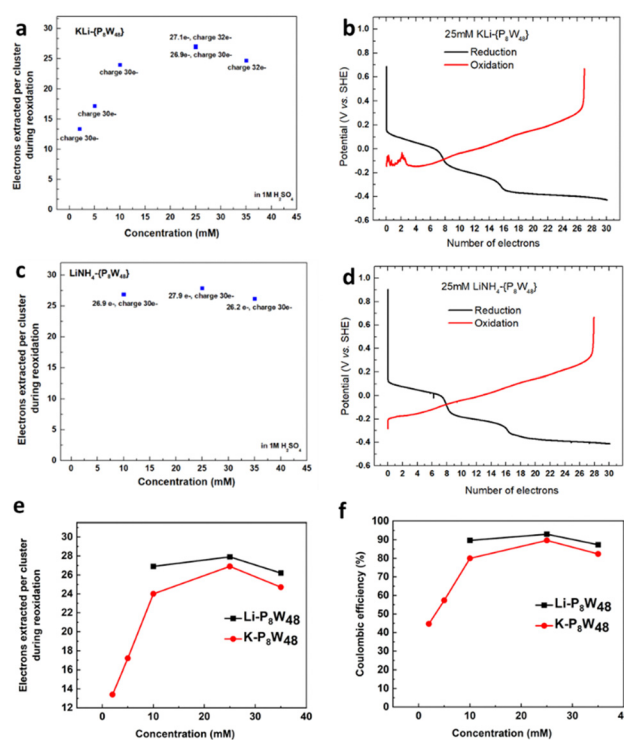

Fig. 3 Reversible multi-electron redox chemistry of [H₇P₈W₄₈O₁₈₄]³³⁻. (a) Relationship between KLi-{P₈W₄₈} concentration and the number of electrons that can be extracted from a reduced solution. The number of electrons used to reduce the KLi-{P₈W₄₈} was 30/32 per cluster. 2 mM, 5 mM and 10 mM are under room temperature; 25 mM and 35 mM are under 70 °C. (b) Representative 27 e⁻ reduction/reoxidation curves of a 25 mM solution of KLi-{P₈W₄₈}, 1 M H₂SO₄ was used as supporting electrolyte and a current density of ±25 mA cm⁻² was applied. (c) Relationship between LiNH₄-{P₈W₄₈} concentration and the number of electrons that can be extracted from a reduced solution. (d) Representative 28 e⁻ reduction/reoxidation curves of a 25 mM solution of LiNH₄-{P₈W₄₈}. In (b) and (d), a current density of ±25 mA cm⁻² was applied. A comparison of KLi-{P₈W₄₈} and Li(NH₄)-{P₈W₄₈}: (e) electrons extracted vs. concentration; (f) coulombic efficiency (the total charge extracted out of the total charge put into the POM solutions) vs. concentration.

carefully, there is an extra step appearing around 28–32 e⁻, so for the following experiment we charged 30 e⁻ per cluster, whereby a normal reoxidation curve was observed. KLi-{P₈W₄₈} showed an increased electron storage ability with an increase in concentration from 2 mM, 5 mM, 10 mM to 25 mM (heating was applied from 25 mM due to the solubility limit under room temperature), when charging 30 e⁻ per cluster, to a maximum of 26.9 e⁻. We then tried to charge more (32 e⁻ per cluster) into this system, the performance did not increase significantly. Increasing the concentration to 35 mM, the performance dropped to 24.7 e⁻. The best performance was achieved at 25 mM with 26.9 e⁻ retrieved after charging by 30 e⁻, shown in Fig. 3b. Similarly, for LiNH₄-{P₈W₄₈} among 10 mM, 25 mM and 35 mM, the concentration of 25 mM still displays the best performance (27.9 e⁻ out of 30 e⁻, Fig. 3c, d and Table S8 and Fig. S22, ESI†). Overall the LiNH₄ salt slightly outperformed the KLi salt at all concentrations measured (Fig. 3e).

2606 | Energy Environ. Sci., 2023, **16**, 2603–2610

This journal is © The Royal Society of Chemistry 2023

Comparison of Li-{P₂W₁₈}, Li-{P₅W₃₀} and LiNH₄-{P₈W₄₈}

We compared the electrochemical performance of Li-{P_2W_{18}}, Li-{P_5W_{30}} and LiNH₄-{P_8W_{48}} in terms of extracted number of electrons and coulombic efficiency *versus* concentration for a more comprehensive understanding, shown in Fig. 4a and b. From these two figures, we can see the electron storage ability of POMs is affected by concentration of POMs and their structure among {P_2W_{18}}, {P_5W_{30}} and {P_8W_{48}}. The electron storage ability for these three POMs shows both similarities and differences. In terms of similarities, the electron storage ability of them is all dependent on: (1) the concentration of POMs, (2) the nature of the counter cations and (3) the supporting electrolyte pH or proton concentration.

Factors influencing performance

The concentration effect for the large clusters P_5W_{30} and P_8W_{48} is more complex than for P_2W_{18}, whereby increasing concentration leads to a continuous increase in performance. Instead optimal performance is observed at 10 mM for P_5W_{30} and 25 mM for P_8W_{48}, although the region between these two concentrations is relatively flat for both (Fig. 4b). For the larger POMs cation concentration increases more rapidly with increasing POM concentration leading to differences in the protonation/metalation equilibrium which occurs through POM hydrolysis in aqueous media (Fig. 4d and Fig. S26, ESI†).[33] These factors lead to an electron storage performance limit, and even lower performance due to the reduced precipitates which can form during this reduction/reoxidation process, affecting mass transfer in the flow system.
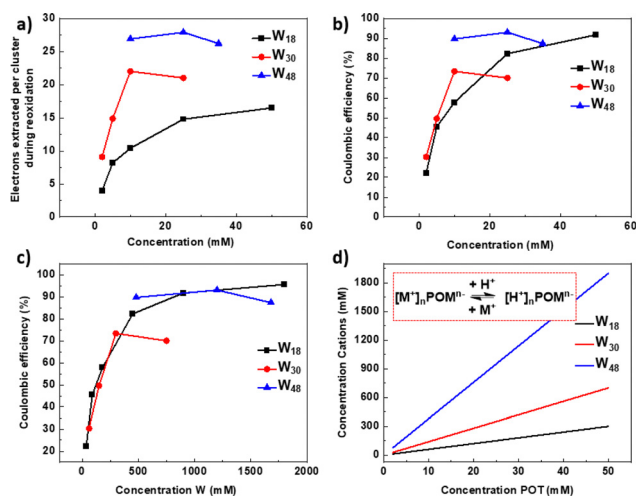

Fig. 4 A comparison of electrochemical performance between Li-{P_2W_{18}}, Li-{P_5W_{30}} and LiNH₄-{P_8W_{48}}. (a) Electrons extracted *vs.* concentration (b) coulombic efficiency *vs.* concentration of polyoxotungstate (POT) (For W_{18}, charge 18 e^-; for W_{30}, charge 30 e^-; for W_{48}, charge 30 e^-, per cluster) (the data for W_{18} are from our prior work[16]). (c) Coulombic efficiency *vs.* concentration of W. (d) Variation of total non-protic counter ions with increasing cluster concentration for the three POMs compared herein. Inset: POM hydrolysis equilibrium between metalation and protonation.

The concentration also affects the impact of different counterions on performance. At low concentration protonation predominates over metalation, particularly for larger, more highly charged cations. Mass Spectrometry data of the two W_{30} salts in both acid and water shows that the potassium salt becomes more protonated than the lithium salt in solution at the same concentration (Fig. S4, S9, S23, S24 and Tables S3, S4, S9, S10, ESI†). This difference in protonation can potentially alter the ability of the POM to stabilise a high charge upon reduction through aggregation. As concentration increases the equilibrium shifts towards metalation, as described above. As such, at high concentration lithium salts show increased performance over Na⁺ and K⁺ salts for all of our POTs (W_{18}, W_{30} and W_{48}). For {P_8W_{48}}, as both of the samples here have mixed counter cations (K⁺ and Li⁺, Li⁺ and NH₄⁺), it is hard to analyse the specific effect of a single cation. Mass spectrometry showed poor solubility upon the water dilution required for injection, however we can observe several broad peaks in the envolopes expected for each of the salts. Exemplar spectral windows and simulated patterns for proposed salts can be found in Fig. S41–S43 (ESI†). Importantly, the performance for the Li–(NH₄)– salt is higher at all concentrations for this cluster.

For coulombic efficiency (Fig. 4b), both {P_5W_{30}} and {P_8W_{48}} showed an advantage over {P_2W_{18}} at low POM concentration (< 20 mM), but for {P_2W_{18}}, the coulombic efficiency continues to increase, approaching 100% when concentration reaches 100 mM. It is interesting to note that normalising for W concentration allows us to observe that all three clusters follow a similar efficiency trajectory (Fig. 4c). Regarding the utilization ratio of W atoms (the ratio of W metal centres which are redox-active for storing electrons among all W atoms in the structure), {P_5W_{30}} still showed an advantage at low concentration, but at concentrations higher than 25 mM the advantage of {P_2W_{18}} begins to emerge; {P_8W_{48}} has the lowest utilization rate of W, only part of W in the structure are redox active and participate in the reduction/oxidation process. (Fig. S25, ESI†)

NMR and mass spectrometry studies

NMR and mass spectrometry next allowed us to probe the effect of concentration and reduction/oxidation on speciation, specifically the cation–anion interaction in solution.[29] Normally ⁷Li NMR shows a sharper signal than ³⁹K NMR, so here we use Li-{P_5W_{30}} as an example to study changes in the samples with varying concentration and reduction state through ⁷Li and ¹H NMR spectroscopy. Firstly, 10 mM of Li-{P_5W_{30}} was studied in 1 M D_2SO_4, and both the ⁷Li and ¹H NMR of original, reduced, and re-oxidized POM solutions were monitored and illustrated in Fig. 5a. Before treatment Li-{P_5W_{30}} resonates at around −0.32 ppm in the ⁷Li spectrum reflecting the mass spectra which show a mixture of lithium and proton cations for the POM in solution (See Fig. S28, ESI†). After reduction, it shifted downfield by +0.06 ppm indicating a decrease in paramagnetic shielding of the lithium ion upon coordination to the POM over solvation[29] (mass spec suggests all of the fourteen available lithium ions are coordinated). (Tables S12 and S14, ESI†).
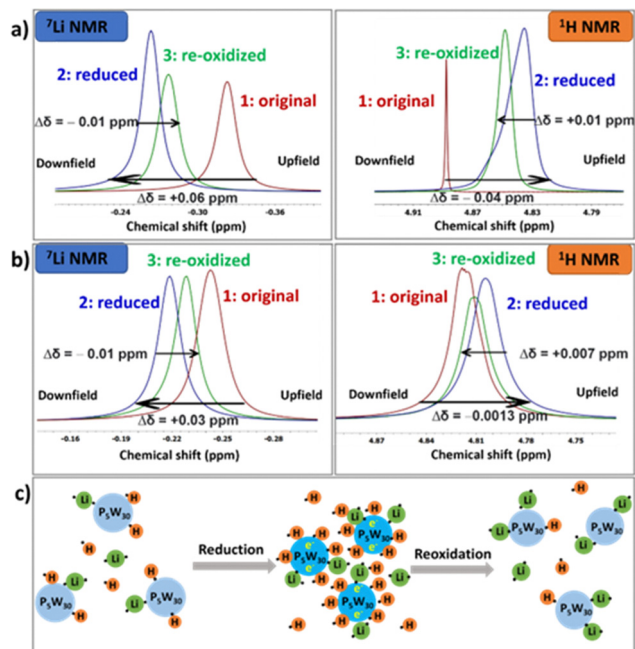
This journal is © The Royal Society of Chemistry 2023

Energy Environ. Sci., 2023, **16**, 2603–2610 | **2607**

Paper

Fig. 5 ^{7}Li and ^{1}H NMR study (a) 10 mM of Li-$\{P_5W_{30}\}$ in 1 M D_2SO_4 charge 30 e$^-$; (b) 10 mM of Li-$\{P_5W_{30}\}$ in 1 M H_2SO_4 charge 20 e$^-$; (c) schematic diagram of protonation/aggregation (reduction and reoxidation process)

Li orbitals are overlapping with the POM oxo ligand orbitals which is also consistent with our previous work.[17] Meanwhile, we monitored ^{1}H NMR and an opposite trend compared to ^{7}Li NMR was observed. The peak around 4.8 ppm represents the protons from H_2O (or HOD) which in D_2SO_4 solution is in equilibrium with DH_2O^+ meaning an intermediate resonance representing the relative position of this equilibrium is observed. After reduction, the acidic protons (deuterons) are bound to the POM oxo ligands shifting this equilibrium and resulting in a more upfield resonance for the H_2O/HOD protons. The reoxidation process of both ^{7}Li and ^{1}H showed an opposite trend as the reduction process, but crucially the resonances did not return to the original peak position. (Fig. S26, ESI†) This is due to the fact that production of H_2 from the system reduces the concentration of H^+ which shifts the equilibrium towards the formation of H_2O/HOD (see performance limit section). This altered speciation upon reduction can provide some explanation of the differences in the CV curves shown in Fig. 1d, if we assume the Li- and K- salts have different metalation levels.

Besides ^{1}H and ^{7}Li NMR, we also monitored ESI-MS and GC for this study and found there is an extra peak on ^{31}P NMR at −11.03 ppm after reoxidation (Fig. S27, ESI†), showing the possible partial decomposition of the cluster. From the ESI-MS spectrum, the re-oxidized $\{P_5W_{30}\}$ has extra peaks at 1091.69 and 1454.92 m/z, compared with the original and reduced one. These two peaks can be assigned as species of $[H_2P_2W_{18}O_{62}]^{4-}$ and $[H_3P_2W_{18}O_{62}]^{3-}$, which is consistent with the β-Dawson as shown in NMR spectrum (Fig. S29, ESI†). At the same time, the flow cell test result shows 11.8 e$^-$ are extracted after the POM has been charged 30 e$^-$ (See Fig. S30, ESI†), which is much less than using H_2SO_4 as solvent (22.0 e$^-$). Samples of the reduced and reoxidised POM in H_2SO_4 showed

no extra peaks in the ESI-MS meaning this degradation may occur due to the different rate of reaction of deuterons and protons in electrochemical kinetics. To further confirm the NMR chemical shift trends on ^{7}Li and ^{1}H, we ran an electrochemical test, charging 20 e$^-$ of Li-$\{P_5W_{30}\}$ in 1 M H_2SO_4, and the results are shown in Fig. 5b. Similar trends on both ^{7}Li and ^{1}H were observed here albeit with a smaller change in chemical shift in both ^{7}Li and ^{1}H spectra due to the lower charge on the POM. An illustration of this process is shown in Fig. 5c.

We also investigated both the ^{7}Li and ^{1}H NMR for the original solution with varied concentration from 2 mM, 5 mM, 10 mM, 25 mM to 50 mM for LiCl, $Li_6\{P_2W_{18}\}$, $Li_{14}\{P_5W_{30}\}$ and Li_{17}-$(NH_4)_{21}\{P_8W_{48}\}$ (Fig. S31–35, ESI†). While no change in the shift was observed for LiCl over the range (Fig. S31, ESI†) a shift of ^{7}Li NMR to downfield was observed when increasing the concentration of all the POMs. This observation supports our assertions above about the effect of increasing alkali metal concentration upon the protonation/metalation equilibrium (effectively decreasing POM hydrolysis). The upfield peak shift in the ^{1}H NMR spectrum with an increase in POM concentration is consistent with a similar observation for Li salts in aqueous solution.[34]

Performance limit analysis

From above electrochemical results, we found that both $\{P_5W_{30}\}$ and $\{P_8W_{48}\}$ have an electron extraction limit which is lower than the number of tungsten atoms in the cluster, unlike $\{P_2W_{18}\}$ which is able to release 17.2 electrons per cluster, with a coulombic efficiency of 96%. Neither $\{P_5W_{30}\}$ nor $\{P_8W_{48}\}$ can store 30 e$^-$/48 e$^-$ per cluster respectively with $\{P_5W_{30}\}$ storing a maximum of 23 e$^-$ per cluster, while $\{P_8W_{48}\}$ can store 28 e$^-$ per cluster. The first possible reason for this performance limit could be POM decomposition during this reduction/reoxidation process. During the electrochemical test, we found that when charging 48 e$^-$ per cluster into $\{P_8W_{48}\}$ the discharge curve rapidly decreased, likely due to degradation of the POM. Secondly, when comparing the structures of the three POMs, we found that the $\{WO_6\}$ polyhedra could be either edge-sharing or corner-sharing with their neighbours. In $\{P_2W_{18}\}$ all of the W atoms are in edge sharing polyhedra whereas in $\{P_5W_{30}\}$ this number is only 20 and $\{P_8W_{48}\}$ has 32 edge-sharing polyhedra. Edge sharing polyhedra are known to undergo reduction more easily than their corner sharing counterparts.[35] Hence a higher barrier to reduction of the corner sharing could limit our ability to charge the cluster. Another possible factor, which may work in concert with the prior issue, could be competitive hydrogen evolution within the electrochemical potential range utilised here.

POM decomposition

We utilised ^{31}P NMR and ESI-MS to study the performance limit of Li-$\{P_5W_{30}\}$ by charging 20, 24 and 30 electrons per cluster respectively into Li-$\{P_5W_{30}\}$ and monitoring the structure change for the original, reduced and re-oxidized POMs of each. At each of the three charging levels only $[NaP_5W_{30}O_{110}]^{14-}$ is observed, indicating there is no decomposition occurring in the experiment (Fig. 6 and Fig. S24, S29, S30, ESI†).
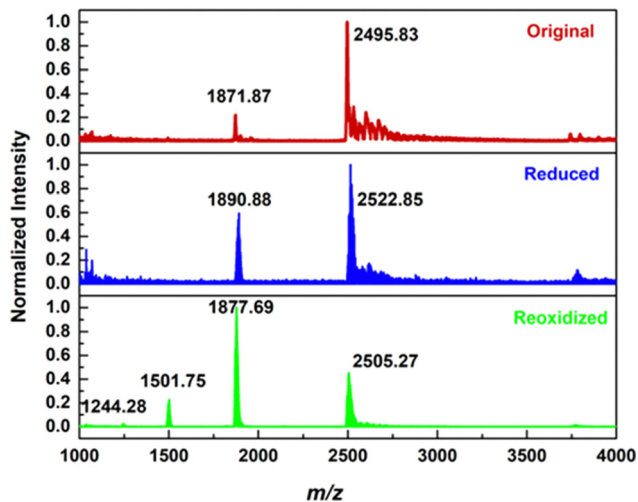
Fig. 6 A typical mass spectrum of sample of the polyoxometalate solution taken from a 10 mM solution of Li-$\{P_5W_{30}\}$ that was (a) original (b) reduced by 30 e$^-$ (c) re-oxidized and then injected into the mass spectrometer (after dilution with degassed methanol). The reduced sample was taken out immediately after charging finished and protected with Ar to avoid oxidation by air, before injection it was also diluted with degassed methanol.

Hydrogen evolution vs. W edge-sharing effect

To analyse for hydrogen evolution and the edge sharing effect we designed a series of three experiments, observing the coulombic efficiency and detection of H$_2$. If the edge sharing effect is the principal reason for the performance limit, then when we charge to 20 e$^-$ we expect to see 100% coulombic efficiency while if we charge to more than 20 e$^-$ we expect to observe hydrogen formation. However, if, no matter how many electrons are added, the coulombic efficiency is always the same (or similar), then hydrogen is formed under all circumstances and the performance limit is caused by unavoidable hydrogen generation.

The electrochemical result and gas analysis for this series of experiment are shown in Table 1. When charged to 30 e$^-$, 22 e$^-$ was extracted and with H$_2$ detected; when charged to 24 e$^-$, less electrons (16.4 e$^-$) were extracted with H$_2$ detected (Fig. S36, ESI†); when charged to 20 e$^-$, a significantly lower number of electrons (14.8 e$^-$) were released out (Fig. S37, ESI†), with H$_2$ still detected. This demonstrates that the performance limit of Li-$\{P_5W_{30}\}$ is due to unavoidable hydrogen generation rather than the edge-sharing effect. At the same time, we also monitored the structure change (through ESI-MS and ^{31}P NMR) for reduced and oxidized ones for charging 20 and 24 e$^-$.

Consistent results were obtained; no decomposition was observed. (See Fig. S38–S40 and Table S16–S19, ESI†). The reason for this unavoidable hydrogen generation is possibly related to the degree of protonation, the structure of the POM/coordination environment of the W, the charge density of the reduced species and the pH of the battery solution.[16]

Conclusions

This work shows that polyoxotungstate clusters like $M_{14}[NaP_5W_{30}O_{110}]$ (M = K$^+$, Li$^+$) and $M_{33}[H_7P_8W_{48}O_{184}]$ (M = K$^+$, Li$^+$ and NH$_4^+$) can achieve very high proton-electron storage capacities in aqueous solution. $\{P_5W_{30}\}$ can store up to 23 e$^-$ and $\{P_8W_{48}\}$ can store up to 28 e$^-$ per cluster, which is the best electron storage ability reported to date for a single molecule.

However, unlike previously reported $\{P_2W_{18}\}$ increasing concentration improves storage ability only up to around 10 mM (P_5W_{30})–25 mM (P_8W_{48}) whereupon the rapidly increasing concentration of cations may impede the ability of the clusters to aggregate through proton bridges. Using acidic electrolyte media can mitigate this effect to a degree and stabilise the POM. At low concentration heavy alkali metal salts (e.g. K) show increased storage likely due to cluster hydrolysis however these are surpassed by more electropositive metal salts (e.g. Li) as concentration and thus metalation increases. The performance limit in coulombic efficiency for these clusters is caused by unavoidable hydrogen generation. In this regard this work helps understand how polyoxometalates might be exploited for flow batteries and how clusters with greater stability and even higher capacities may be designed.

Author contributions

L. C. conceived the idea, and L. C and T. Z designed the project. T. Z synthesized $\{P_5W_{30}\}$ (including all physical characterization), conducted all electrochemistry tests and analysis of $\{P_5W_{30}\}$ and $\{P_8W_{48}\}$, conducted all NMR, MS and GC study of $\{P_5W_{30}\}$ for mechanisms study and relevant analysis, analysed all data together, and wrote the paper; N. L. B contributed on NMR and MS discussion and analysis and helped write the paper; G. C helped with building up the flow cell and contributed on GC measurement; B. K synthesized $\{P_8W_{48}\}$ and finished physical characterization of $\{P_8W_{48}\}$; D-L. L contributed on single crystal XRD characterization and analysis.

Conflicts of interest

There are no conflicts to declare.

Acknowledgements

Table 1 A comparison of battery performance and hydrogen detection of Li-$\{P_5W_{30}\}$ charge to different electrons (30, 24 and 20 e$^-$ per molecule)

	Electrons input	Electrons output	Coulombic efficiency (%)	H$_2$ detected
Li-$\{P_5W_{30}\}$ 10 mM in 1 M H$_2$SO$_4$	30.0	22.0	73	Yes
	24.0	16.4	68	Yes
	20.0	14.8	74	Yes

References

1 M. R. Horn, A. Singh, S. Alomari, S. Goberna-Ferrón, R. Benages-Vilau, N. Chodankar, N. Motta, K. Ostrikov, J. MacLeod, P. Sonar, P. Gomez-Romero and D. Dubal, *Energy Environ. Sci.*, 2021, **14**, 1652–1700.

2 Z. Li and Y.-C. Lu, *Adv. Mater.*, 2020, **32**, 2002132.

3 W. Wang, Q. Luo, B. Li, X. Wei, L. Li and Z. Yang, *Adv. Funct. Mater.*, 2013, **23**, 970–986.

4 J. Zhang, G. Jiang, P. Xu, A. Ghorbani Kashkooli, M. Mousavi, A. Yu and Z. Chen, *Energy Environ. Sci.*, 2018, **11**, 2010–2015.

5 M. L. Perry, K. E. Rodby and F. R. Brushett, *ACS Energy Lett.*, 2022, **7**, 659–667.

6 X.-P. Gao and H.-X. Yang, *Energy Environ. Sci.*, 2010, **3**, 174–189.

7 D. L. Long, E. Burkholder and L. Cronin, *Chem. Soc. Rev.*, 2007, **36**, 105–121.

8 D. L. Long, R. Tsunashima and L. Cronin, *Angew. Chem., Int. Ed.*, 2010, **49**, 1736–1758.

9 H. D. Pratt, N. S. Hudak, X. Fang and T. M. Anderson, *J. Power Sources*, 2013, **236**, 259–264.

10 J. Friedl, F. L. Pfanschilling, M. V. Holland-Cunz, R. Fleck, B. Schricker, H. Wolfschmidt and U. Stimming, *Clean Energy*, 2019, **3**, 278–287.

11 J. P. Launay, *Phys. Chem. Chem. Phys.*, 1976, **38**, 807–816.

12 C. Boskovic, M. Sadek, R. T. C. Brownlee, A. M. Bond and A. G. Wedd, *J. Chem. Soc., Dalton Trans.*, 2001, 187–196, DOI: **10.1039/b006264m**.

13 D. M. Way, A. M. Bond and A. G. Wedd, *Inorg. Chem.*, 1997, **36**, 2826–2833.

14 H. Wang, S. Hamanaka, Y. Nishimoto, S. Irle, T. Yokoyama, H. Yoshikawa and K. Awaga, *J. Am. Chem. Soc.*, 2012, **134**, 4918–4924.

15 E. Sánchez-Díez, E. Ventosa, M. Guarnieri, A. Trovò, C. Flox, R. Marcilla, F. Soavi, P. Mazur, E. Aranzabe and R. Ferret, *J. Power Sources*, 2021, **481**, 228804.

16 J. J. Chen, M. D. Symes and L. Cronin, *Nat. Chem.*, 2018, **10**, 1042–1047.

17 J.-J. Chen, L. Vilà-Nadal, A. Solé-Daura, G. Chisholm, T. Minato, C. Busche, T. Zhao, B. Kandasamy, A. Y. Ganin, R. M. Smith, I. Colliard, J. J. Carbó, M. P. Josep, M. Nyman and L. Cronin, *J. Am. Chem. Soc.*, 2022, **144**, 8951–8960.

18 M. H. Alizadeh, S. P. Harmalker, Y. Jeannin, J. Martin-Frere and M. T. Pope, *J. Am. Chem. Soc.*, 1985, **107**, 2662–2669.

19 A. Hayashi, T. Haioka, K. Takahashi, B. S. Bassil, U. Kortz, T. Sano and M. Sadakane, *Z. Anorg. Allg. Chem.*, 2015, **641**, 2670–2676.

20 A. Hayashi, M. N. K. Wihadi, H. Ota, X. Lopez, K. Ichihashi, S. Nishihara, K. Inoue, N. Tsunoji, T. Sano and M. Sadakane, *ACS Omega*, 2018, **3**, 2363–2373.

21 R. Contant and A. Teze, *Inorg. Chem.*, 1985, **24**, 4610–4614.

22 M. Segado, M. Nyman and C. Bo, *J. Phys. Chem. B*, 2019, **123**, 10505–10513.

23 A. Misra, K. Kozma, C. Streb and M. Nyman, *Angew. Chem., Int. Ed.*, 2020, **59**, 596–612.

24 V. A. Grigoriev, D. Cheng, C. L. Hill and I. A. Weinstock, *J. Am. Chem. Soc.*, 2001, **123**, 5292–5307.

25 A. B. Gunnarsdottir, C. V. Amanchukwu, S. Menkin and C. P. Grey, *J. Am. Chem. Soc.*, 2020, **142**, 20814–20827.

26 K. A. See, M. Leskes, J. M. Griffin, S. Britto, P. D. Matthews, A. Emly, A. Van der Ven, D. S. Wright, A. J. Morris, C. P. Grey and R. Seshadri, *J. Am. Chem. Soc.*, 2014, **136**, 16368–16377.

27 E. W. Zhao, T. Liu, E. Jonsson, J. Lee, I. Temprano, R. B. Jethwa, A. Wang, H. Smith, J. Carretero-Gonzalez, Q. Song and C. P. Grey, *Nature*, 2020, **579**, 224–228.

28 D. Sures, M. Segado, C. Bo and M. Nyman, *J. Am. Chem. Soc.*, 2018, **140**, 10803–10813.

29 D. J. Sures, S. A. Serapian, K. Kozma, P. I. Molina, C. Bo and M. Nyman, *Phys. Chem. Chem. Phys.*, 2017, **19**, 8715–8725.

30 E. G. Bloor and R. G. Kidd, *Can. J. Chem.*, 1972, **50**, 3926–3930.

31 M. J. Turo, L. Chen, C. E. Moore and A. M. Schimpf, *J. Am. Chem. Soc.*, 2019, **141**, 4553–4557.

32 B. Keita, Y. W. Lu, L. Nadjo and R. Contant, *Electrochem. Commun.*, 2000, **2**, 720–726.

33 N. I. Gumerova and A. Rompel, *Chem. Soc. Rev.*, 2020, **49**, 7568–7601.

34 S. Cai, T. Bai, H. Chen, W. Fang, Z. Xu, H. Lai, T. Huang, H. Xu, X. Chu, J. Ling and C. Gao, *J. Phys. Chem. Lett.*, 2020, **11**, 303–310.

35 R. I. Buckley and R. J. H. Clark, *Coord. Chem. Rev.*, 1985, **65**, 167–218.

2610 | *Energy Environ. Sci.*, 2023, **16**, 2603–2610

This journal is © The Royal Society of Chemistry 2023